ISSN 1070-4280, Russian Journal of Organic Chemistry, 2016, Vol. 52, No. 12, pp. 1822–1829. © Pleiades Publishing, Ltd., 2016.
Original Russian Text © D.A. Lomov, S.N. Lyashchuk, M.G. Abramyants, 2016, published in Zhurnal Organicheskoi Khimii, 2016, Vol. 52, No. 12, pp. 1828–1836.

Design and Synthesis of Imidazo[4,5-*c*]pyridine Derivatives as Promising Aurora Kinase A (AURKA) Inhibitors

D. A. Lomov,* S. N. Lyashchuk, and M. G. Abramyants

Litvinenko Institute of Physical Organic Chemistry, ul. Rozy Lyuksemburg 70, Donetsk, 83000 Ukraine
**e-mail: lomov_dmitrii@mail.ru*

Received June 28, 2016

Abstract—Computer simulation at the PM7 level of theory of the structures of imidazo[4,5-*c*]pyridine derivatives (deaza analogs of purines) and their complexes with Aurora kinase A (AURKA) indicated prospects for their use as potential AURKA inhibitors in the treatment of oncological diseases. A number of new compounds of the selected imidazo[4,5-*c*]pyridine series, for which the highest inhibitory activity against AURKA was predicted, were synthesized in high yields for further biological testing.

DOI: 10.1134/S1070428016120198

About 6 million new cancer occurrences is registered worldwide annually, and this situation remains unchanged over the past two decades. Although cancer and other malignant oncological diseases constitute 5–10% of all cases of somatic diseases, they follow next to cardiovascular disorders with respect to mortality.

In 1994–1997, three new kinases overexpressed in cancer have been identified in dividing cells of warm-blooded by PCR (polymerase chain reaction) [1]. Aurora kinases belong to a small family of serine/threonine protein kinases, which includes three enzymes: Aurora kinase A (AURKA), Aurora kinase B (AURKB), and Aurora kinase C (AURKC) [2–4]. These enzymes are involved in the most important molecular events in all stages of cell mitosis [5]. Considerable increase of the concentration of AURKA and AURKB induces nondisjunction, so that some cells degrade and die, while the others degenerate to tumor cells with a high probability [6]. It was shown experimentally that increased concentrations of Aurora kinases largely determine the development of many types of stomach, liver, and rectal cancers, some breast and pancreatic cancers, as well as of leukemia [2]. Thus, detection of increased AURKA and AURKB contents is an important diagnostic test for carcinogenic process or precancer state [7].

The new drug hesperadin (**1**) has recently been introduced into clinical practice; it is capable of suppressing excess activity of AURKA and AURKB in tumor tissues [8]. Study of the mechanism of hesperadin-induced inhibition of the catalytic activity of these enzymes has shown [9] that the drug blocks active site of the enzyme. At present, some leading pharmaceutical companies perform extensive search for new Aurora kinase inhibitors with the goal of creating new-generation anticancer drugs [10]. Currently known Aurora kinase inhibitors are represented by various heterocyclic structures; some compounds, e.g., **2**–**6**, are now under clinical trials [4, 11].

In recent years, while searching for new kinase inhibitors, researchers' attention has been focused on imidazo[4,5-*b*]pyridine derivatives [12, 13]. Compounds **5** and **6** showed a pronounced inhibitory effect against AURKA, and the magnitude of this effect may change by 1–2 orders upon insignificant structural modification of the inhibitor molecule [14, 15]. These data indicate high selectivity of binding to the enzyme active site. Analogous studies of imidazo[4,5-*c*]pyridine derivatives as Aurora kinase inhibitors have not been reported in the literature. Taking into account that imidazo[4,5-*b*]pyridine and imidazo[4,5-*c*]pyridine are the closest structural analogs, the latter are expected to exhibit similar biological properties, in particular with respect to various kinases.

The inhibitory activity of a series of imidazo[4,5-*c*]pyridine derivatives against AURKA was quantitatively assessed by computational methods (*in silico*), followed by directed synthesis of compounds with the highest predicted activity.

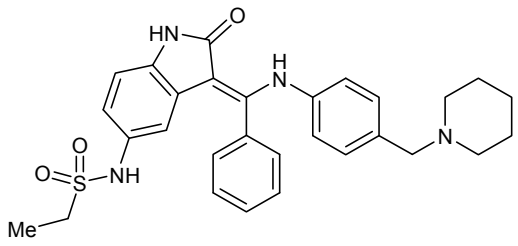

1

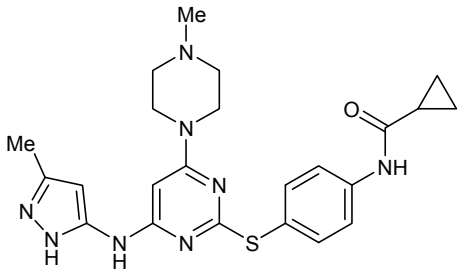

2, VX-680

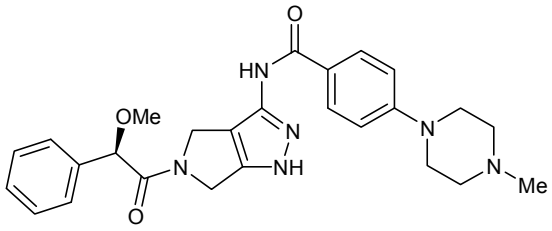

3, PHA-739358

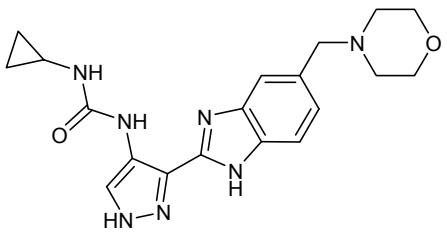

4, AT-9283

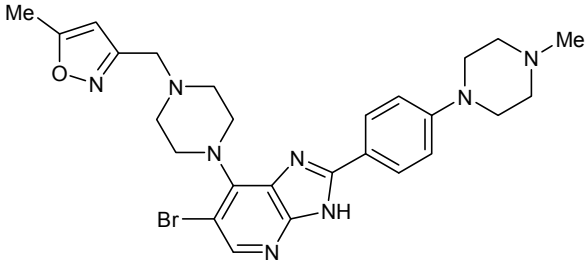

5, CCT-137690

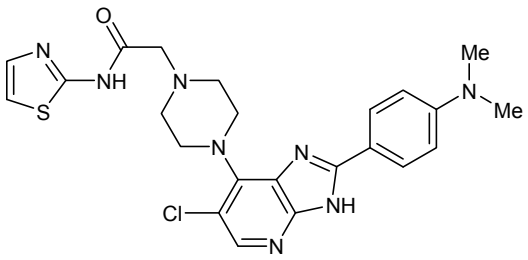

6, CCT-129202

In the first step, as subjects for the study we selected a sample consisting of 24 imidazo[4,5-*c*]pyridines **7**–**30** as potential ligands for AURKA inhibition. The choice was based on the drug likeness approach implying that structurally related compounds may possess similar biological properties. In our case, the closest analogs of compounds **7**–**30** are imidazo-[4,5-*b*]pyridine derivatives [12–15].

An empirical approach based on Lipinski's rules [16] has found wide application in the design of new drugs since it allows considerable contraction of the series of compounds to be studied. According to Lipinski's rules, a compound could be a drug if its molecule contains no more than 5 donor centers capable of forming hydrogen bonds (OH and NH groups), no more than 10 hydrogen bond acceptor centers (N, O), and no more than 15 nonterminal freely rotating bonds; furthermore, its molecular weight should be lower than 500, and the octanol–water partition coefficient log*P* should be lower than 5. All compounds **7**–**30** conform to Lipinski's rules, and there are some "reserves" regarding the molecular composition and properties, which provide the possibility of obtaining more complex analogs through variation and modification of substituents therein.

An alternative approach to prediction of potential effect of compounds on cellular processes is provided by Molinspiration on-line service (version 2004.1) [17]. This software is based on a huge, continuously updated database, and it makes it possible not only to determine whether a compound fits Lipinski's rules but also to predict *in silico* with a high probability some

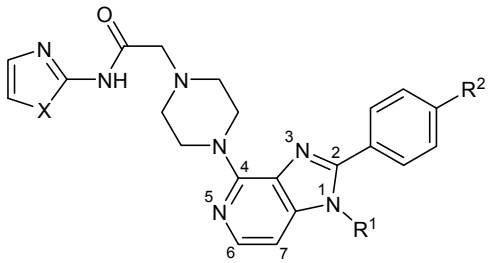

7–**30**

7, **10**, **13**, **16**, **19**, **22**, **25**, **28**, X = NH; **8**, **11**, **14**, **17**, **20**, **23**, **26**, **29**, X = S; **9**, **12**, **15**, **18**, **21**, **24**, **27**, **30**, X = O; **7**–**9**, **13**–**15**, **19**–**21**, **25**–**27**, R^1 = H; **10**–**12**, **16**–**18**, **22**–**24**, **28**–**30**, R^1 = Me; **7**–**12**, R^2 = NMe_2; **13**–**18**, R^2 = MeO; **19**–**24**, R^2 = Cl; **25**–**30**, R^2 = Br.

biological properties of imidazo[4,5-*c*]pyridine derivatives. The results of the Molinspiration predictions for compounds **7**–**30** are given in Table 1.

All compounds **7**–**30** could both activate and inhibit proteases (IP –0.15 to 0.20), modulate and demodulate ion channels (MIC –0.21 to 0.20), and inhibit cellular enzymes in total (IE 0.02–0.40); however, the probability of these properties is not high (≤40%). They are also capable of acting as medium-strength nuclear receptor activators (NRL –0.17 to –0.51) and inhibit transmembrane receptors (GPCR varies over a wide range from 0.06 to 0.58). The most probable property is the ability to inhibit kinases (IK 0.23–0.56).

By semiempirical quantum chemical calculations at the PM7 level of theory [18] using MOPAC2012 version 15.281W [19] we obtained more detailed information on the structure and electronic properties of molecules **7**–**30** and their complexes with AURKA. The calculated parameters given in Table 2 may be used as descriptors in the assessment of the inhibitory activity of the ligands against enzymes.

The dipole moments of **7**–**30** vary over a wide range (4.66–12 D) and strongly depend on the substituents in the imidazopyridine fragment. The negative charge is localized on the nitrogen atom of that fragment, and variation of the substituents exerts an appreciable effect only on the N^1 atom: $q(N^1)$ –0.432 to –0.295, $q(N^2)$ –0.437 to –0.366, $q(N^3)$ –0.550 to –0.509 a.u. The positive charge is localized on the carbon atoms. The absolute electronegativities EN 4.05–4.81 and the absolute hardnesses η 7.26–7.81 calculated from the HOMO and LUMO energies [20] are typical of nitrogen-containing heterocyclic systems capable of being involved in donor–acceptor interac-

Table 1. Some biological activities[a] of compounds **7**–**30** predicted by Molinspiration (version 2004.1)

Compound no.	IK	MIC	GPCR	NRL	IP	IE
7	0.53	0.06	0.42	–0.25	0.04	0.22
8	0.44	–0.07	0.17	–0.39	–0.06	0.12
9	0.56	0.16	0.54	–0.17	0.14	0.39
10	0.39	–0.04	0.39	–0.26	–0.03	0.17
11	0.27	–0.17	0.13	–0.39	–0.13	0.06
12	0.39	0.05	0.49	–0.18	0.07	0.32
13	0.49	0.02	0.41	–0.28	0.02	0.20
14	0.40	–0.10	0.15	–0.42	–0.09	0.10
15	0.52	0.13	0.53	–0.19	0.12	0.38
16	0.35	–0.07	0.37	–0.29	–0.05	0.15
17	0.23	–0.21	0.10	–0.42	–0.15	0.04
18	0.35	0.02	0.47	–0.20	0.05	0.31
19	0.52	0.08	0.46	–0.29	0.04	0.22
20	0.43	–0.05	0.19	–0.44	–0.08	0.12
21	0.56	0.20	0.58	–0.20	0.14	0.40
22	0.37	–0.02	0.41	–0.30	–0.04	0.16
23	0.25	–0.16	0.14	–0.44	–0.15	0.05
24	0.37	0.08	0.52	–0.21	0.07	0.33
25	0.50	0.03	0.38	–0.37	–0.02	0.19
26	0.41	–0.10	0.11	–0.51	–0.13	0.09
27	0.54	0.14	0.51	–0.28	0.09	0.37
28	0.35	–0.08	0.34	–0.37	–0.10	0.13
29	0.23	–0.21	0.06	–0.51	0.20	0.02
30	0.35	0.02	0.45	–0.28	0.01	0.30

[a] IK stands for kinase inhibition; MIC stands for ion channel modulation; GPCR (G protein-coupled receptors) stands for ligand binding to seven-transmembrane receptors; NRL stands for ligand binding to nuclear receptors; IP stands for protease inhibition; IE stands for enzyme inhibition. Negative sign of the biological activity indices indicates activation of the respective bioprocess.

Table 2. Heats of formation, dipole moments, effective charges on some atoms, and frontier orbital energies of compounds **7**–**30**, calculated by the PM7 method (MOPAC2012)

Comp. no.	ΔH^f, kJ/mol	μ, D	Effective charges on atoms, a.u.						Energy, eV	
			N^1	C^2	N^3	C^4	N^5	C^6	HOMO	LUMO
7	339.77	6.71	–0.422	0.299	–0.406	0.408	–0.517	0.139	–7.91	–0.36
8	353.27	7.24	–0.423	0.313	–0.437	0.409	–0.518	0.143	–8.12	–0.37
9	262.32	10.82	–0.432	0.292	–0.401	0.402	–0.527	0.147	–8.05	–0.50
10	357.65	9.91	–0.316	0.267	–0.384	0.419	–0.546	0.149	–7.90	–0.21
11	348.10	8.08	–0.306	0.298	–0.439	0.410	–0.518	0.138	–8.05	–0.25
12	259.52	12.00	–0.316	0.271	–0.390	0.406	–0.528	0.143	–8.06	–0.25
13	165.86	6.97	–0.427	0.267	–0.376	0.413	–0.531	0.147	–8.22	–0.67
14	223.52	9.22	–0.429	0.272	–0.394	0.403	–0.519	0.151	–8.34	–0.83
15	76.35	9.15	–0.428	0.267	–0.385	0.408	–0.529	0.154	–8.31	–0.70
16	145.39	7.32	–0.310	0.253	–0.383	0.410	–0.524	0.141	–8.24	–0.57
17	219.72	9.84	–0.316	0.264	–0.400	0.398	–0.509	0.141	–8.29	–0.63
18	72.78	9.60	–0.312	0.252	–0.385	0.408	–0.529	0.148	–8.22	–0.52
19	302.08	4.58	–0.419	0.244	–0.369	0.413	–0.524	0.153	–8.44	–1.08
20	375.39	7.42	–0.420	0.246	–0.379	0.406	–0.522	0.157	–8.46	–1.16
21	228.38	7.45	–0.420	0.242	–0.372	0.412	–0.530	0.160	–8.42	–1.05
22	321.79	6.22	–0.305	0.221	–0.366	0.428	–0.550	0.161	–8.14	–0.88
23	310.34	5.89	–0.295	0.255	–0.422	0.414	–0.518	0.145	–8.29	–0.72
24	224.04	8.50	–0.304	0.229	–0.376	0.411	–0.530	0.153	–8.32	–0.92
25	356.91	4.66	–0.418	0.242	–0.369	0.413	–0.521	0.153	–8.43	–1.09
26	430.14	7.42	–0.419	0.244	–0.378	0.407	–0.523	0.158	–8.46	–1.17
27	283.22	7.50	–0.420	0.241	–0.373	0.411	–0.529	0.159	–8.42	–1.06
28	352.25	5.54	–0.303	0.228	–0.372	0.413	–0.524	0.146	–8.33	–0.93
29	367.43	5.70	–0.296	0.256	–0.422	0.414	–0.519	0.145	–8.29	–0.75
30	278.86	8.55	–0.304	0.227	–0.376	0.411	–0.530	0.152	–8.32	–0.92

tions. According to the X-ray diffraction data for AURKA complexes with different inhibitors, Aurora kinase is an enzyme containing 402 amino acid residues and N- and C-terminal domains.

The AURKA complexes with potential inhibitors **7**–**30** were calculated in several steps. In the first step, the ligand was removed from the active site of the known AURKA complex with 4-{[2-(4-{[(4-fluorophenyl)carbonyl]amino}-1*H*-pyrazol-3-yl)-1*H*-benzimidazol-6-yl]methyl}morpholin-4-ium cation [21], whose structure was determined by X-ray analysis (RCSB Protein Data Bank ID: 2W1C), using Accelrys Discovery Studio 3.5 program. The structure of the protein molecule thus obtained was taken as the initial approximation and was optimized by PM7 semiempirical quantum chemical calculations (MOPAC2012; MOZYME module for the calculation of protein molecules and complex macromolecular assemblies was applied). The corresponding inhibitor with an IK index of larger than 0.35 (which rendered it sufficiently active) was then placed into the active site, and the structure of the complex was optimized. All enthalpies of formation (Table 2) were calculated for the optimized structures.

As an example, Fig. 1 shows the calculated structure of the AURKA complex with compound **11**. The inhibitor molecule binds to the enzyme active site and is held thereon, thus leading to inactivation of the kinase in the cell division process. The stability of the protein–inhibitor complex is determined by the energy of its formation (exothermic process). Furthermore, ligand docking induces change of the secondary protein structure in the regions adjacent to the active site, which should also favor enzyme deactivation.

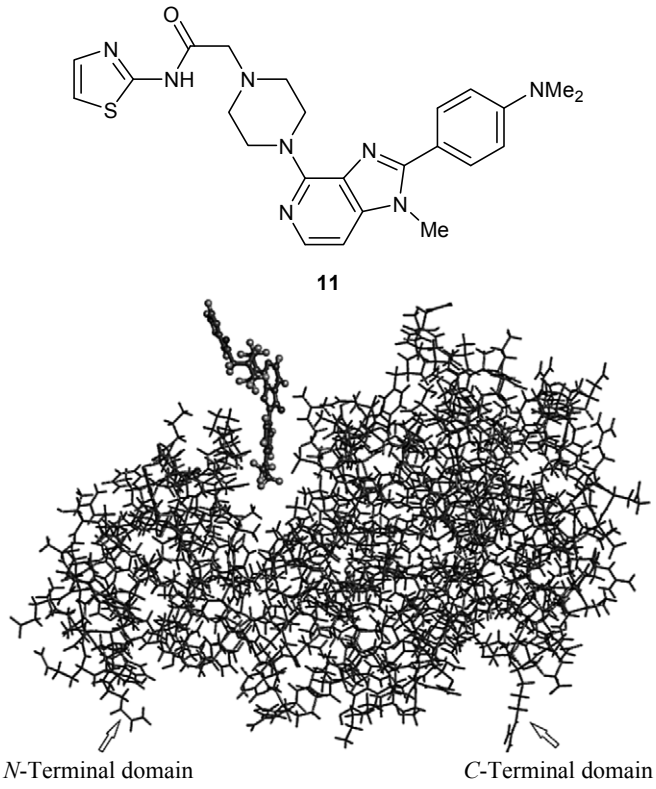

Fig. 1. Optimized structure of the Aurora kinase A complex with inhibitor **11** bound to the active site.

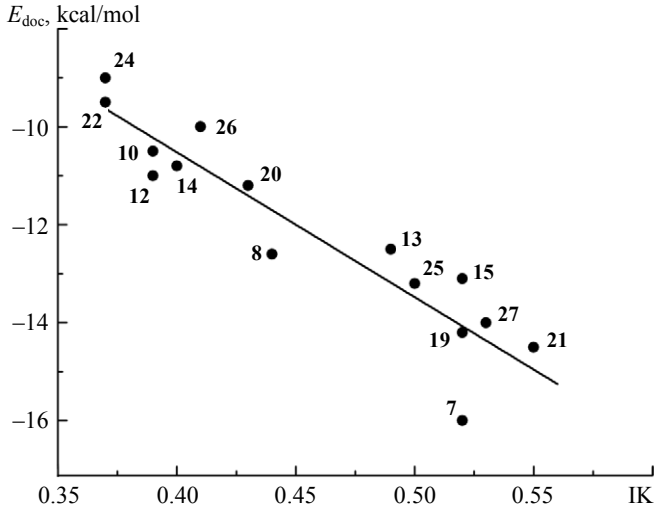

Fig. 2. Correlation of the docking energy (E_{doc}) with the kinase inhibitory activity (IK) of compounds **7**–**10**, **12**–**15**, **19**–**22**, and **24**–**27**, calculated by Molinspiration program (version 2004.1).

The docking energy E_{doc} for individual compounds was calculated as the difference in the enthalpy of formation of the complex $\Delta H^f_{AURKA–L}$ and the sum of the enthalpies of formation of unbound AURKA (ΔH^f_{AURKA}) and the corresponding ligand ΔH^f_L (1):

$$E_{doc} = \Delta H^f_{AURKA–L} – (\Delta H^f_{AURKA} + \Delta H^f_L). \quad (1)$$

The calculated protein–ligand docking energy is linearly related to the kinase inhibition index IK determined by Molinspiration 2004.1 (Fig. 2) through Eq. (2):

$$E_{doc} = (1.31\pm1.36) – (29.57\pm2.92)\text{IK};$$
$$r^2 = 0.871,\ s_0 = 8.32. \quad (2)$$

Our results indicated that all compounds **7**–**30** are capable of binding to the AURKA active site to greater or lesser extent. This especially applies to those possessing no methyl group on the nitrogen atom of the imidazopyridine fragment. Elongation of the alkyl substituent strongly reduces E_{doc} in absolute value due to considerable steric hindrances to approach of the inhibitor molecule to the active site and holding it therein.

For further biological testing we synthesized six imidazo[4,5-*c*]pyridine derivatives **7**, **9**, **15**, **19**, **21**, and **27** for which the highest inhibitory activity against AURKA was predicted. The key intermediate products for the synthesis of these compounds were 2-chloropyridine-3,4-diamine (**31**) [22], *N*-(1*H*-imidazol-2-yl)-2-(piperazin-1-yl)acetamide (**32**), and *N*-(1,3-oxazol-2-yl)-2-(piperazin-1-yl)acetamide (**33**). Acetamides **32** and **33** were synthesized in 72–83% yield by heating *N*-imidazolyl- and *N*-oxazolylchloroacetamides **34** and **35** with piperazine hydrochloride (prepared *in situ*) in ethanol (Scheme 1). In the ^{1}H NMR spectra of **32** and **33**, signals of the piperazine fragment appeared as two singlets as δ 2.70–2.83 and 3.03–3.12 ppm.

2-Chloropyridine-3,4-diamine (**31**) reacted with *para*-substituted benzoic acids **36**–**39** in phosphoryl chloride at 130–140°C to give 4-chloro-2-phenyl-3*H*-imidazo[4,5-*c*]pyridines **40**–**43** in 50–64% yield (Scheme 2). Compounds **40**–**43** displayed in the ^{1}H NMR spectra signals from protons of the pyridine ring as two doublets at δ 7.57–7.62 and 7.93–8.25 ppm, and protons of the *para*-substituted benzene ring resonated at δ 6.83–7.81 and 8.04–8.24 ppm.

By reacting 4-chloro-2-phenylimidazo[4,5-*c*]pyridine derivatives **40**–**43** with acetamides **32** and **33** on heating in ethanol in the presence of triethylamine we obtained compounds **7**, **9**, **15**, **19**, **21**, and **27** in 52–78% yield (Scheme 3). Analogous compounds were synthesized in [23] under similar conditions. In the ^{1}H NMR spectra of **7**, **9**, **15**, **19**, **21**, and **27** we observed doublets at δ 7.58–8.28 and 7.59–7.94 ppm due to protons in the pyridine ring, doublets at δ 6.81–

Scheme 1.

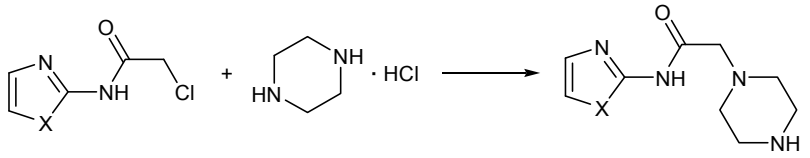

34, **35** **32**, **33**

32, **34**, X = NH; **32**, **35**, X = O.

Scheme 2.

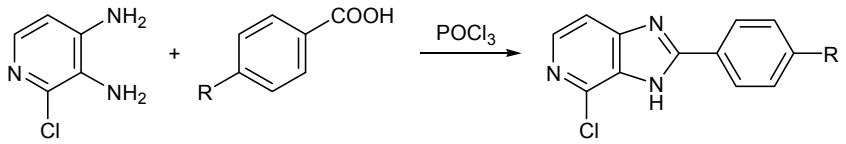

31 **36–39** **40–43**

36, **40**, R = Me_2N; **37**, **41**, R = MeO; **38**, **42**; R = Cl; **39**, **43**, R = Br.

Scheme 3.

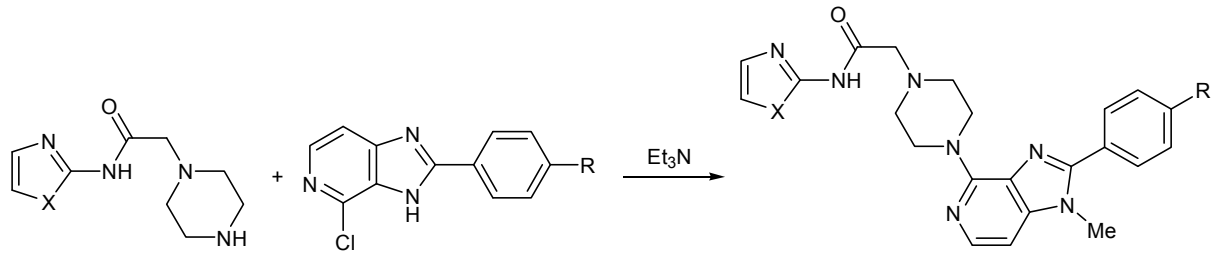

32, **33** **40–43** **7**, **9**, **15**, **19**, **21**, **27**

7, **19**, **32**, X = NH; **9**, **15**, **21**, **27**, **33**, X = O; **7**, **9**, **40**, R = Me_2N; **15**, **41**, R = MeO; **19**, **21**, **42**, R = Cl; **27**, **43**, R = Br.

7.81 and 8.06–8.26 ppm due to protons of the benzene ring, and signals of protons in the piperidine and azole rings.

Thus, computer simulation of deaza analogs of purine bases, imidazo[4,5-*c*]pyridine derivatives, and their complexes with AURKA indicates prospects of their use as potential inhibitors of this key enzyme for oncological practice.

EXPERIMENTAL

The ^{1}H NMR spectra were recorded on a Bruker Avance II 400 spectrometer at 400 MHz using DMSO-d_6 as solvent and tetramethylsilane as internal standard. The purity of the isolated compounds was checked by TLC on Silufol UV-254 plates using methanol–chloroform (1 : 10) as eluent; spots were visualized by treatment with iodine vapor or under UV light.

Compounds 32 and 33 (*general procedure*). Piperazine hexahydrate, 10 mmol, was dissolved in 10 mL of propan-1-ol, 10 mmol of piperazine dihydrochloride monohydrate was added, and the mixture was heated with stirring until it became homogeneous. A solution of chloroacetamide **34** or **35** in 10 mL of propan-1-ol was added to the resulting solution of piperazine hydrochloride, and the mixture was heated for 2 h at 80–90°C and cooled. The precipitate of piperazine dihydrochloride was filtered off and washed on a filter with 5 mL of propan-1-ol. The filtrate was evaporated to 1/3 of the initial volume and filtered while hot. Compounds **32** and **33** crystallized from the filtrate on cooling.

***N*-(1*H*-Imidazol-2-yl)-2-(piperazin-1-yl)acetamide (32).** Yield 83%, mp 107–109°C. ^{1}H NMR spectrum, δ, ppm: 2.83 s (4H, C**H**$_2$NHC**H**$_2$), 3.12 s (4H, CH_2NCH_2), 3.44 (2H, CH_2), 7.12 s (2H, 4-H, 5-H), 11.92 br.s (1H, NH). Found, %: C 51.61; H 7.25; N 33.41. $C_9H_{15}N_5O$. Calculated, %: C 51.66; H 7.23; N 33.47.

***N*-(1,3-Oxazol-2-yl)-2-(piperazin-1-yl)acetamide (33).** Yield 72%, mp 79–81°C. ^{1}H NMR spectrum, δ, ppm: 2.70 s (4H, C**H**$_2$NHC**H**$_2$), 3.03 s (4H, CH_2NCH_2), 3.32 (2H, CH_2), 7.38 d (1H, 4-H, *J* =

4.0 Hz), 7.73 d (1H, 5-H, J = 4.0 Hz), 11.92 br.s (1H, NH). Found, %: C 51.37; H 6.72; N 26.47. $C_9H_{14}N_4O_2$. Calculated, %: C 51.42; H 6.71; N 26.65.

Compounds 40–43 (*general procedure*). A mixture of 3 mmol of 2-chloropyridine-3,4-diamine **31** and 3 mmol of *para*-substituted benzoic acid **36**–**39** in 4 mL of phosphoryl chloride was heated for 3–3.5 h at 130–135°C. Vigorous evolution of hydrogen chloride was observed. When the reaction was complete, excess $POCl_3$ was distilled off, the residue was treated with cold water, and the precipitate was filtered off, dried, and recrystallized from appropriate solvent.

4-(4-Chloro-3*H*-imidazo[4,5-*c*]pyridin-2-yl)-*N*,*N*-dimethylaniline (40). Yield 64%, mp 245–247°C (from PrOH). ^{1}H NMR spectrum, δ, ppm: 3.01 s [6H, $N(CH_3)_2$], 6.83 d (2H, 3′-H, 5′-H, J = 8.0 Hz), 7.62 d (1H, 7-H, J = 8.0 Hz), 8.04 d (2H, 2′-H, 6′-H, J = 8.0 Hz), 8.25 d (1H, 6-H, J = 8.0 Hz). Found, %: C 61.60; H 4.82; N 20.51. $C_{14}H_{13}ClN_4$. Calculated %: C 61.65; H 4.80; N 20.54.

4-Chloro-2-(4-methoxyphenyl)-3*H*-imidazo-[4,5-*c*]pyridine (41). Yield 54%, mp 163–165°C (from H_2O). ^{1}H NMR spectrum, δ, ppm: 3.85 s (3H, OCH_3), 7.15 d (2H, 3′-H, 5′-H, J = 8.0 Hz), 7.57 d (1H, 7-H, J = 8.0 Hz), 8.09 d (1H, 6-H, J = 8.0 Hz), 8.18 d (2H, 2′-H, 6′-H, J = 8.0 Hz). Found, %: C 60.10; H 3.92; N 16.14. $C_{13}H_{18}ClN_3O$. Calculated, %: C 60.12; H 3.88; N 16.18.

4-Chloro-2-(4-chlorophenyl)-3*H*-imidazo[4,5-*c*]-pyridine (42). Yield 53%, mp 243–245°C (from PrOH). ^{1}H NMR spectrum, δ, ppm: 7.57 d (1H, 7-H, J = 8.0 Hz), 7.68 d (2H, 3′-H, 5′-H, J = 8.0 Hz), 7.93 d (1H, 6-H, J = 8.0 Hz), 8.24 d (2H, 2′-H, 6′-H, J = 8.0 Hz). Found, %: C 54.53; H 2.69; N 15.87. $C_{12}H_7Cl_2N_3$. Calculated, %: C 54.57; H 2.67; N 15.91.

2-(4-Bromophenyl)-4-chloro-3*H*-imidazo[4,5-*c*]-pyridine (43). Yield 50%, mp 268–270°C (from PrOH). ^{1}H NMR spectrum, δ, ppm: 7.60 d (1H, 7-H, J = 8.0 Hz), 7.81 d (2H, 3′-H, 5′-H, J = 8.0 Hz), 8.13 d (1H, 6-H, J = 8.0 Hz), 8.15 d (2H, 2′-H, 6′-H, J = 8.0 Hz). Found, %: C 46.68; H 2.31; N 13.58. $C_{12}H_7BrClN_3$. Calculated, %: C 46.71; H 2.29; N 13.62.

Condensation of compounds 40–43 with acetamides 32 and 33 (*general procedure*). A mixture of 0.4 mmol of compound **40**–**43**, 0.4 mmol of acetamide **32 or 33**, 0.5 mL of propan-1-ol, and 0.3 mL of triethylamine was heated for 4–5 h at 110–120°C. The mixture was evaporated to dryness, the residue was treated with water, and the precipitate was filtered off, dried, and recrystallized from appropriate solvent.

2-(4-{2-[(4-Dimethylamino)phenyl]-1*H*-imidazo-[4,5-*c*]pyridin-4-yl}piperazin-1-yl)-*N*-(1*H*-imidazol-2-yl)acetamide (7). Yield 62%, mp 183–185°C (from EtOH). ^{1}H NMR spectrum, δ, ppm: 2.85 s (4H, CH_2NCH_2), 3.03 s [6H, $N(CH_3)_2$], 3.10 s (4H, CH_2NCH_2), 3.41 (2H, CH_2), 6.81 d (2H, 3′-H, 5′-H, J = 8.0 Hz), 7.10 s (2H, 4″-H, 5″-H), 7.60 d (1H, 7-H, J = 8.0 Hz), 8.07 d (2H, 2′-H, 6′-H, J = 8.0 Hz), 8.23 d (1H, 6-H, J = 8.0 Hz). Found, %: C 61.98; H 6.16; N 28.27. $C_{23}H_{27}N_9O$. Calculated, %: C 62.01; H 6.11; N 28.30.

2-(4-{2-[(4-Dimethylamino)phenyl]-1*H*-imidazo-[4,5-*c*]pyridin-4-yl}piperazin-1-yl)-*N*-(1,3-oxazol-2-yl)acetamide (9). Yield 63%, mp 152–154°C (from EtOH). ^{1}H NMR spectrum, δ, ppm: 2.75 s (4H, CH_2NCH_2), 2.99 s [6H, $N(CH_3)_2$], 3.05 s (4H, CH_2NCH_2), 3.37 (2H, CH_2), 6.87 d (2H, 3′-H, 5′-H, J = 8.0 Hz), 7.37 d (1H, 4″-H, J = 4.0 Hz), 7.63 d (1H, 7-H, J = 8.0 Hz), 7.75 d (1H, 5″-H, J = 4.0 Hz), 8.06 d (2H, 2′-H, 6′-H, J = 8.0 Hz), 8.28 d (1H, 6-H, J = 8.0 Hz). Found, %: C 61.49; H 5.91; N 25.01. $C_{23}H_{26}N_8O_2$. Calculated, %: C 61.87; H 5.87; N 25.10.

2-{4-[2-(4-Methoxyphenyl)-1*H*-imidazo[4,5-*c*]-pyridin-4-yl]piperazin-1-yl}-*N*-(1,3-oxazol-2-yl)-acetamide (15). Yield 78%, mp 193–195°C (from PrOH). ^{1}H NMR spectrum, δ, ppm: 2.72 s (4H, CH_2NCH_2), 3.03 s (4H, CH_2NCH_2), 3.37 (2H, CH_2), 3.85 s (3H, OCH_3), 7.14 d (2H, 3′-H, 5′-H, J = 8.0 Hz), 7.37 d (1H, 4″-H, J = 4.0 Hz), 7.59 d (1H, 7-H, J = 8.0 Hz), 7.75 d (1H, 5″-H, J = 4.0 Hz), 8.04 d (1H, 6-H, J = 8.0 Hz), 8.14 d (2H, 2′-H, 6′-H, J = 8.0 Hz). Found, %: C 60.90; H 5.39; N 21.44. $C_{22}H_{23}N_7O_3$. Calculated, %: C 60.96; H 5.35; N 22.62.

2-{4-[2-(4-Chlorophenyl)-1*H*-imidazo[4,5-*c*]-pyridin-4-yl]piperazin-1-yl}-*N*-(1*H*-imidazol-2-yl)-acetamide (19). Yield 52%, mp 207–209°C (from PrOH). ^{1}H NMR spectrum, δ, ppm: 2.83 s (4H, CH_2NCH_2), 3.12 s (4H, CH_2NCH_2), 3.47 (2H, CH_2), 7.16 s (2H, 4″-H, 5″-H), 7.72 d (2H, 3′-H, 5′-H, J = 8.0 Hz), 7.94 d (1H, 6-H, J = 8.0 Hz), 8.26 d (2H, 2′-H, 6′-H, J = 8.0 Hz), 7.58 d (1H, 7-H, J = 8.0 Hz). Found, %: C 57.65; H 4.87; N 25.58. $C_{21}H_{21}ClN_8O$. Calculated, %: C 57.73; H 4.84; N 25.65.

2-{4-[2-(4-Chlorophenyl)-1*H*-imidazo[4,5-*c*]-pyridin-4-yl]piperazin-1-yl}-*N*-(1,3-oxazol-2-yl)-acetamide (21). Yield 52%, mp 173–175°C (from PrOH). ^{1}H NMR spectrum, δ, ppm: 2.69 s (4H, CH_2NCH_2), 3.03 s (4H, CH_2NCH_2), 3.35 (2H, CH_2), 7.37 d (1H, 4″-H, J = 4.0 Hz), 7.59 d (1H, 7-H, J = 8.0 Hz), 7.68 d (2H, 3′-H, 5′-H, J = 8.0 Hz), 7.71 d

(1H, 5″-H, J = 4.0 Hz), 7.95 d (1H, 6-H, J = 8.0 Hz), 8.23 d (2H, 2′-H, 6′-H, J = 8.0 Hz). Found, %: C 57.56; H 4.62; N 22.37. $C_{21}H_{20}ClN_7O_2$. Calculated, %: C 57.60; H 4.60; N 22.39.

2-{4-[2-(4-Bromophenyl)-1*H*-imidazo[4,5-*c*]pyridin-4-yl]piperazin-1-yl}-*N*-(1,3-oxazol-2-yl)acetamide (27). Yield 78%, mp 212–214°C (from PrOH). ^{1}H NMR spectrum, δ, ppm: 2.72 s (4H, CH_2NCH_2), 3.05 s (4H, CH_2NCH_2), 3.34 (2H, CH_2), 7.37 d (1H, 4″-H, J = 4.0 Hz), 7.62 d (1H, 7-H, J = 8.0 Hz), 7.73 d (1H, 5″-H, J = 4.0 Hz), 7.81 d (2H, 3′-H, 5′-H, J = 8.0 Hz), 8.11 d (2H, 2′-H, 6′-H, J = 8.0 Hz), 8.15 d (1H, 6-H, J = 8.0 Hz). Found, %: C 52.21; H 4.23; N 20.29. $C_{21}H_{20}BrN_7O_2$. Calculated, %: C 52.29; H 4.18; N 20.33.

REFERENCES

1. Sen, S., Zhou, H., and White, R.A., *Oncogene*, 1997, vol. 14, p. 2195.
2. Libertini, S., Abagnale, A., Passaro, C., Botta, G., and Portella, G., *Recent Pat. Anti-Cancer Drug Discovery*, 2010, vol. 5, p. 219.
3. Zhang, J., Yang, P.L., and Gray, N.S., *Nat. Rev. Cancer*, 2001, vol. 9, p. 28.
4. Dar, A.A., Goff, L.W., Majid, Sh., Berlin, J., and El-Rifai, W., *Mol. Cancer Ther*., 2010, vol. 9, p. 268.
5. Murata-Hori, M., Tatsuka, M., and Wang, Y.L., *Mol. Biol. Cell*, 2002, vol. 13, p. 1099.
6. Gürtler, U., Tontsch-Grunt, U., Jarvis, M., Zahn, S.K., Boehmelt, G., Quant, J., Adolf, G.R., and Solca, F., *J. Clin. Oncol*., 2010, vol. 28, p. 1363.
7. Sorrentino, R., Libertini, S., Pallante, P.L., Troncone, G., Palombini, L., Bavetsias, V., Spalletti-Cernia, D., Laccetti, P., Linardopoulos, S., Chieffi, P., Fusco, A., and Portella, G., *J. Clin. Endocrinol. Metab*., 2005, vol. 90, p. 928.
8. Ladygina, N.G., Latsis, R.V., and En, T., *Biomed. Khim*., 2005, vol. 51, p. 170.
9. Sessa, F., Mapelli, M., Ciferri, C., Tarricone, C., Areces, L.B., Schneider, Th.R., Stukenberg, P.T., and Musacchio, A., *Mol. Cell*, 2005, vol. 18, p. 379.
10. Koroleva, E.V., Ignatovich, Zh.I., Sinyutich, Yu.V., and Gusak, K.N., *Russ. J. Org. Chem*., 2016, vol. 52, p. 139.
11. Yan, A., Wang, L., Xu, Sh., and Xu, J., *Drug Discovery Today*, 2011, vol. 16, p. 261.
12. Bavetsias, V., Large, J.M., Sun, Ch., Bouloc, N., Kosmopoulou, M., Matteucci, M., Wilsher, N.E., Martins, V., Reynisson, J., Atrash, B., Faisal, A., Urban, F., Valenti, M., de Haven Brandon, A., Box, G., Raynaud, F.I., Workman, P., Eccles, S.A., Bayliss, R., Blagg, J., Linardopoulos, S., and McDonald, E., *J. Med. Chem*., 2010, vol. 53, p. 5213.
13. Lan, P., Chen Wan-Na, and Chen Wei-Min, *Eur. J. Med. Chem*., 2011, vol. 46, p. 77.
14. Bavetsias, V., Crumpler, S., Sun, Ch., Avery, S., Atrash, B., Faisal, A., Moore, A.S., Kosmopoulou, M., Brown, N., Sheldrake, P.W., Bush, K., Henley, A., Box, G., Valenti, M., de Haven Brandon, A., Raynaud, F.I., Workman, P., Eccles, S.A., Bayliss, R., Linardopoulos, S., and Blagg, J., *J. Med. Chem*., 2012, vol. 55, p. 8721.
15. Bavetsias, V., Faisal, A., Crumpler, S., Brown, N., Kosmopoulou, M., Joshi, A., Atrash, B., Pérez-Fuertes, Y., Schmitt, J.A., Boxall, K.J., Burke, R., Sun, C., Avery, S., Bush, K., Henley, A., Raynaud, F.I., Workman, P., Bayliss, R., Linardopoulos, S., and Blagg, J., *J. Med. Chem*., 2013, vol. 56, p. 9122.
16. Lipinski, C.A., Lombardo, F., Dominy, B.W., and Feeney, P.J., *Adv. Drug Delivery Rev*., 1997, vol. 23, p. 3.
17. *Molinspiration ver.2004.1: program (on-line service)*: Molinspiration Cheminformatics, Slovak Rep., 2015. http://www.molinspiration.com
18. Stewart, J.J.P., *J. Mol. Model*., 2013, vol. 19, p. 1.
19. Stewart, J.J.P., *MOPAC2012*, Colorado Springs: Stewart Computational Chemistry, 2013. http://openmopac.net
20. Pearson, R.G., *Chemical Hardness*, Weinheim: Wiley-VCH, 1997.
21. Howard, S., Berdini, V., Boulstridge, J.A., Carr, M.G., Cross, D.M., Curry, J., Devine, L.A., Early, T.R., Fazal, L., Gill, A.L., Heathcote, M., Maman, S., Matthews, J.E., Mcmenamin, R.L., Navarro, E.F., O'Brien, M.A., O'Reilly, M., Rees, D.C., Reule, M., Tisi, D., Williams, G., Vinkovic, M., and Wyatt, P.G., *J. Med. Chem*., 2009, vol. 52, p. 379.
22. Bremer, O.J., *Justus Liebigs Ann. Chem*., 1935, vol. 518, p. 274.
23. Svertilova, I.A., Smolyar, N.N., and Yutilov, Yu.M., *Ukr. Khim. Zh*., 1996, vol. 62, p. 64.